

Deletion of the gene encoding G₀/G₁ switch protein 2 (*G0s2*) alleviates high-fat-diet-induced weight gain and insulin resistance, and promotes browning of white adipose tissue in mice

Wissal El-Assaad · Karim El-Kouhen · Amro H. Mohammad · Jieyi Yang · Masahiro Morita · Isabelle Gamache · Orval Mamer · Daina Avizonis · Nicole Hermance · Sander Kersten · Michel L. Tremblay · Michelle A. Kelliher · Jose G. Teodoro

Received: 1 September 2014 / Accepted: 29 September 2014 / Published online: 9 November 2014
© Springer-Verlag Berlin Heidelberg 2014

Abstract

Aims/hypothesis Obesity is a global epidemic resulting from increased energy intake, which alters energy homeostasis and results in an imbalance in fat storage and breakdown. G₀/G₁ switch gene 2 (*G0s2*) has been recently characterised in vitro as an inhibitor of adipose triglyceride lipase (ATGL), the rate-limiting step in fat catabolism. In the current study we aim to functionally characterise *G0s2* within the physiological context of a mouse model.

Electronic supplementary material The online version of this article (doi:10.1007/s00125-014-3429-z) contains peer-reviewed but unedited supplementary material, which is available to authorised users.

W. El-Assaad · K. El-Kouhen · M. Morita · I. Gamache · M. L. Tremblay · J. G. Teodoro (✉)
Goodman Cancer Research Centre, McGill University, Room 616,
1160 Ave des Pins, Montréal, QC H3A 1A3, Canada
e-mail: jose.teodoro@mcgill.ca

A. H. Mohammad · J. Yang · M. L. Tremblay · J. G. Teodoro
Department of Biochemistry, McGill University,
Montréal, QC, Canada

O. Mamer · D. Avizonis
Metabolomics Core Facility, Goodman Cancer Research Centre,
McGill University, Montréal, QC, Canada

N. Hermance · M. A. Kelliher
Department of Cancer Biology, University of Massachusetts,
Worcester, MA, USA

S. Kersten
Nutrition, Metabolism, and Genomics Group, Division of Human
Nutrition, Wageningen University, Wageningen, the Netherlands

J. G. Teodoro
Department of Microbiology and Immunology, McGill University,
Montréal, QC, Canada

Methods We generated a mouse model in which *G0s2* was deleted. The homozygous *G0s2* knockout (*G0s2*^{-/-}) mice were studied over a period of 22 weeks. Metabolic variables were measured including body weight and body composition, food intake, glucose and insulin tolerance tests, energy metabolism and thermogenesis.

Results We report that *G0s2* inhibits ATGL and regulates lipolysis and energy metabolism in vivo. *G0s2*^{-/-} mice are lean, resistant to weight gain induced by a high-fat diet and are glucose tolerant and insulin sensitive. The white adipose tissue of *G0s2*^{-/-} mice has enhanced lipase activity and adipocytes showed enhanced stimulated lipolysis. Energy metabolism in the *G0s2*^{-/-} mice is shifted towards enhanced lipid metabolism and increased thermogenesis. *G0s2*^{-/-} mice showed enhanced cold tolerance and increased expression of thermoregulatory and oxidation genes within white adipose tissue, suggesting enhanced ‘browning’ of the white adipose tissue.

Conclusions/interpretation Our data show that *G0s2* is a physiological regulator of adiposity and energy metabolism and is a potential target in the treatment of obesity and insulin resistance.

Keywords Adipose tissue browning · ATGL · Energy expenditure · *G0s2* · High-fat diet · Insulin resistance · Lipolysis · Obesity · Thermogenesis

Abbreviations

ATGL Adipose triglyceride lipase
BAT Brown adipose tissue
DAG Diacylglycerol
FA Fatty acid
G0S2 G₀/G₁ switch protein 2

H&E	Haematoxylin and eosin
HFD	High-fat diet
HSL	Hormone-sensitive lipase
IPGTT	Intraperitoneal glucose tolerance test
IPITT	Intraperitoneal insulin tolerance test
MAG	Monoacylglycerol
MAGL	Monoacylglycerol lipase
PPAR γ	Peroxisome proliferator-activated receptor γ
RQ	Respiratory quotient
TG	Triacylglycerol
UCP1	Uncoupling protein 1
$\dot{V}O_2$	Oxygen consumption
WAT	White adipose tissue
WT	Wild-type

Introduction

Obesity is recognised as a global epidemic with serious implications for worldwide health. The medical condition is closely associated with several metabolic diseases known as the metabolic syndrome (reviewed in [1]), characterised by dyslipidaemia, hypertension, nonalcoholic fatty liver disease, insulin resistance and others. These metabolic complications brought about by increased fat mass, particularly in the intra-abdominal area, are closely associated with insulin resistance, which subsequently leads to type 2 diabetes [2]. During states of fasting or high energy demand (e.g. exercise), fat stored in adipocytes is mobilised by a series of lipolytic enzymes, leading to the release of NEFA into the circulation. Adipose triglyceride lipase (ATGL) [3–5], the first and rate-limiting enzyme in this series, acts on triacylglycerol (TG) and hydrolyses it into diacylglycerol (DAG). Hormone-sensitive lipase (HSL) [6, 7] and monoacylglycerol lipase (MAGL) further hydrolyse DAG and monoacylglycerol (MAG) leading to NEFA release into the circulation. Increased circulating NEFA levels are strongly associated with insulin resistance and play a major role in the pathogenesis of type 2 diabetes [8]. Thus, lipid homeostasis is governed by genes and signalling molecules responsible for maintaining energy homeostasis.

Despite the importance of lipid and energy homeostasis to human health, these processes are not yet fully understood. Recently, *G0S2* emerged as a potential player in lipid homeostasis regulating the rate-limiting step of lipid catabolism [9]. G α /G β 1 switch protein 2 (G0S2) was shown to directly interact with ATGL and inhibit its catalytic activity [10]. G0S2 is ubiquitously expressed and has been shown to localise to different cellular compartments including endoplasmic reticulum, mitochondria and lipid droplets [9–12]. Moreover, *G0S2* was reported to be a peroxisome proliferator-activated receptor γ (PPAR γ) target gene containing a PPAR response

element [11] and a carbohydrate response element in its promoter [13]. Thus, *G0S2* is emerging as a key regulator of intracellular lipid metabolism but its function has yet to be placed within the physiological context of the whole organism.

In this study, we focused on the metabolic aspects of *G0s2* and its regulation of ATGL in a mouse model in which the *G0s2* gene is deleted. We investigated the role of *G0s2* in lipid metabolism and energy homeostasis in vivo and examined the fate of the released NEFA.

Methods

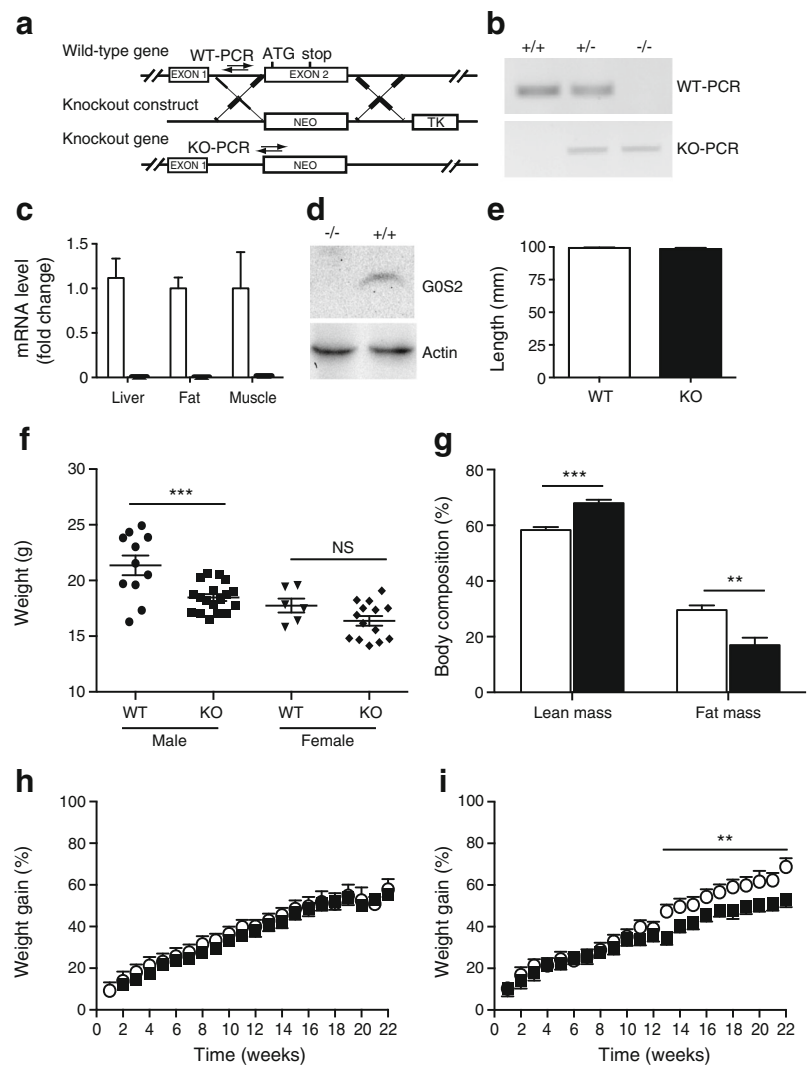
Generation of *G0s2* knockout mice The homozygous *G0s2* knockout (*G0s2*^{-/-}) mice were generated by homologous recombination in embryonic stem cells. A schematic of the targeting strategy is shown in Fig. 1a and additional information is described in electronic supplementary material (ESM Methods). All animal protocols were approved by the Canadian Council on Animal care and the McGill University Animal Care committee. 129SvEv (wild-type [WT]) and *G0s2*^{-/-} mice were housed in a controlled environment at 21°C with a 12 h light/dark cycle and free access to food and water.

Weight studies At 6 weeks of age, mice were placed on either a HFD (24.6% carbohydrates, 21% protein and 54.3% fat on the basis of energy; Harlan Teklad, Toronto, ON, Canada) or a chow diet (60% carbohydrates, 24% protein and 16% fat on the basis of energy; Harlan, Teklad) for 22 weeks. Body weight was measured and recorded on a weekly basis and expressed as percentage of weight gain. At the end of the experiment, mice were killed and tissues were rapidly collected, weighed and either frozen in liquid nitrogen and stored at -80°C or processed for histological analysis.

Adipocyte measurements Histological analyses were performed using haematoxylin and eosin (H&E) stained cross-sectional images using ImageJ software (NIH, Bethesda, MD, USA). More than 1,500 cells on 10 \times images and 9,000 nuclei on 20 \times images were counted manually using the cell counter plugin available on ImageJ from each genotype for white adipose tissue (WAT) and brown adipose tissue (BAT), respectively.

Adipocyte differentiation and lipolysis measurement Pre-adipocytes isolated from 3- to 4-week-old mice were differentiated as described previously [14]. Glycerol (BioVision, Milpitas, CA, USA) and NEFA (Wako Chemicals, Richmond, VA, USA) were measured according to the manufacturer's instructions using appropriate standards. Data were normalised to protein content.

Fig. 1 Effects of *G0s2* deletion on weight gain. **(a)** Schematic representation of the *G0s2* knockout (KO) gene with locations of primers used for genotyping indicated. **(b)** PCR genotyping of *G0s2* WT, heterozygote and KO genes as described in the **Methods**. **(c)** *G0s2* expression levels in liver, fat and muscle tissues of WT (white bars) and KO (black bars) mice. **(d)** G0S2 protein levels in liver lysates. **(e)** Comparison of body length (nose–anus length) of WT and KO mice. **(f)** Comparison of body weights of male and female mice at 6 weeks on chow diet ($n=11$ for WT and 18 for KO male mice; $n=6$ for WT and $n=14$ for female KO mice). **(g)** Body mass composition of 22-week-old male WT and KO mice on chow diet ($n=8$ for WT and 7 for KO mice). **(h, i)** Percentage of weight gain of male WT (white circles) and KO (black squares) mice housed on either chow **(h)** or HFD **(i)** for 22 weeks ($n=8$ for WT mice on both diets; $n=13$ on chow diet and $n=12$ for KO mice on HFD). Data are presented as means \pm SEM. ** $p<0.01$, *** $p<0.001$



Real-time quantitative PCR analysis Real-time quantitative PCR analysis and the primers used are listed in ESM **Methods** and in ESM Table 1.

Statistical analyses Data are presented as means \pm SEM, as calculated by GraphPad Prism (San Diego, CA, USA) software using unpaired two-tailed Student's *t* test. $p<0.05$ was considered significant.

Details of the tolerance tests, in vivo metabolic and thermogenesis measurements, body mass composition, TG content, TG lipase activity, GC-MS and western blot analysis are available in the ESM **Methods**.

Results

G0s2^{-/-} mice are resistant to diet-induced obesity To understand the role of the *G0s2* gene in lipolysis and whole body

metabolism, we generated mice with targeted *G0s2* deletions using homologous recombination (Fig. 1a, b). *G0s2* mRNA and protein levels are shown in Fig. 1c, d. All experiments were performed in the 129SvEv genetic background. The *G0s2*^{-/-} mice were viable and fertile; however, they were leaner than littermate controls (ESM Fig. 1a), with no difference in body length (Fig. 1e). Figure 1f shows weights of mice at 6 weeks of age on a chow diet. Both male and female *G0s2*^{-/-} mice were leaner than littermate controls; however, only in male *G0s2*^{-/-} mice was the reduction in weight statistically significant (21.36 \pm 0.8 g for WT vs 18.47 \pm 0.3 g for *G0s2*^{-/-} mice, $p=0.001$). Analysis of body composition using MRI showed an increase in whole body lean mass and a decrease in fat mass by around 15% and 50%, respectively, in 18-week-old *G0s2*^{-/-} mice compared with WT mice (Fig. 1g). To further elucidate the effects of *G0s2* on body weight, WT and *G0s2*^{-/-} mice were placed either on a chow or HFD and weights were recorded weekly for 22 weeks. There was no difference in weight gain between WT and *G0s2*^{-/-}

mice on the chow diet (Fig. 1b); however, on the HFD $G0s2^{-/-}$ mice were clearly leaner and resistant to obesity induced by the HFD (Fig. 1i and ESM Fig. 1b, c). The resistance to weight gain became apparent at around 12 weeks of HFD feeding and persisted until the end of the experiment. Although 129SvEv background mice are known to be somewhat resistant to diet-induced obesity [15, 16], $G0s2^{-/-}$ male mice showed increased resistance to HFD-induced obesity compared with WT littermates.

Blood chemistry analyses of WT and $G0s2^{-/-}$ mice are shown in Table 1. There were no significant changes in any of the measured variables in either fed or fasted states, including glucose, insulin or TG. Sera TG levels were decreased in knockout mice under HFD conditions but the difference did not achieve statistical significance.

Although no overall differences in NEFA levels were observed, we determined if specific NEFA species were affected. Studies of MAGL have suggested that alterations in lipase activity can lead to differences in the profile of specific NEFA species [17]. We therefore determined if this was also the case in $G0s2^{-/-}$ mice. Fatty acid (FA) profiling using GC-MS on lipids from visceral fat (ESM Fig. 2) was performed but did not show statistical differences between genotypes.

$G0s2^{-/-}$ mice have reduced fat deposition in the liver Analysis of organ weights and morphology showed no significant changes between genotypes under conditions of the chow diet (Fig. 2a); however, under the HFD significant increases were observed in weights of liver and WAT of WT animals that were not apparent in knockout mice (Fig. 2a). Histological analysis of liver sections showed increased fat deposition in the form of lipid droplets in WT mice, which were completely absent in $G0s2^{-/-}$ mice (Fig. 2b). TG levels in livers of WT mice were on average 60% higher than those of the $G0s2^{-/-}$ mice when fed chow diet. Under the HFD, differences in TG levels were even greater, with WT mice

having ~80% more TG relative to knockout mice ($p < 0.0001$; Fig. 2c). Surprisingly, no differences were observed in NEFA levels in liver (Fig. 2d), suggesting that NEFA may be rapidly used or oxidised in $G0s2^{-/-}$ mice. Consistent with the observation showing less fat deposition in livers of $G0s2^{-/-}$ mice, we generally observed reduced expression of genes encoding lipogenic factors such as *Scd1* and *Srebp1c* (also known as *Srebf1*) and elevated levels of lipid oxidative genes (Fig. 2e).

$G0s2^{-/-}$ mice have smaller adipocytes and elevated lipolysis Figure 2a indicated that reduced body mass of the $G0s2^{-/-}$ mice is due primarily to differences in the weight of visceral fat. On HFD, but not chow, the weight of visceral fat was significantly elevated in WT animals relative to $G0s2^{-/-}$ mice. Further analyses of histological sections of visceral fat (Fig. 3a) showed a decrease in the average area of individual adipocytes in $G0s2^{-/-}$ mice (Fig. 3b). This again suggests that in $G0s2^{-/-}$ mice, adipocytes are smaller due to enhanced lipolysis and a decrease in the accumulation of TG. Similar trends were observed with BAT, although the values did not reach statistical significance (Fig. 3a, d). No changes were observed in the size of fat pads between WT and $G0s2^{-/-}$ mice (Fig. 3a, c).

To understand the role of *G0s2* in lipolysis in vivo, we measured TG hydrolase activity in visceral fat from WT and $G0s2^{-/-}$ mice. TG hydrolase activity was significantly higher in $G0s2^{-/-}$ mice than WT littermate controls (about a twofold increase), consistent with *G0S2* being a lipase inhibitor (Fig. 3e) [9, 18]. Moreover, activity was even further enhanced in $G0s2^{-/-}$ mice fed HFD (more than 2.5-fold) compared with WT controls (Fig. 3e). In addition to the increased lipase activity in $G0s2^{-/-}$ mice, ATGL protein levels were also increased under both chow and HFD conditions in $G0s2^{-/-}$ mice (Fig. 3f), suggesting that *G0S2* may inhibit ATGL activity by decreasing steady state levels of the enzyme. No changes were observed in levels of HSL under both diets

Table 1 Plasma levels of glucose, insulin, NEFA, TG, cholesterol and HDL in 22-week-old fed or overnight-fasted male WT and $G0s2^{-/-}$ mice on chow and HFD

Variable	Chow		HFD	
	WT	$G0s2^{-/-}$	WT	$G0s2^{-/-}$
Glucose (mmol/l)	4.8±0.18 (n=8)	4.26±0.18 (n=10)	5.57±0.32 (n=8)	5.8±0.2 (n=11)
Glucose (mmol/l) (fed)	8.3±0.13 (n=8)	8.1±0.12 (n=10)	8.3±0.13 (n=8)	8.3±0.18 (n=10)
Insulin (pmol/l) (fed)	178.5±28 (n=6)	171.5±10.5 (n=6)	490±98 (n=8)	437.5±105 (n=9)
NEFA (mmol/l)	1.41±0.28 (n=8)	1.22±0.16 (n=13)	1.35±0.14 (n=8)	0.94±0.13 (n=12)
TG (mmol/l)	ND	ND	9.23±2.2 (n=7)	8.83±1.1 (n=11)
Cholesterol (mmol/l)	3.6±0.08 (n=6)	3.49±0.15 (n=11)	3.9±0.21 (n=8)	3.9±0.16 (n=12)
HDL-cholesterol (mmol/l)	3.58±0.12 (n=6)	3.4±0.19 (n=11)	4.02±0.16 (n=8)	3.9±0.13 (n=12)

Data are presented as means±SEM (n)

ND, not determined

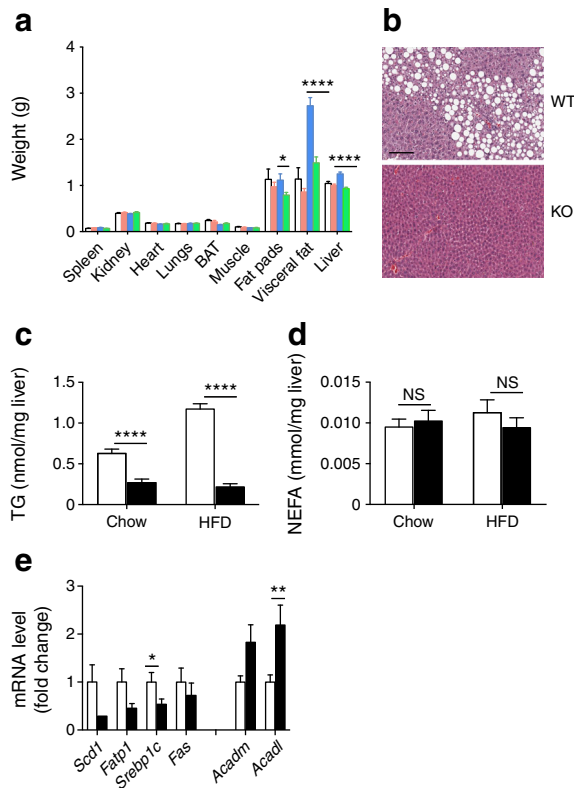


Fig. 2 TG accumulation in livers of $G0s2^{-/-}$ mice. **(a)** Analysis of body organs of WT (white bars) and $G0s2^{-/-}$ (KO) (orange) mice on chow diet and WT (blue) and KO (green) mice on HFD. **(b)** Representative images of H&E staining of liver sections of WT and KO mice on HFD ($n=4$ per genotype). **(c, d)** Liver TG and NEFA levels of WT (white bars) and KO (black bars) mice on chow and HFD. **(e)** Expression analysis of lipogenic and oxidative genes in livers of HFD-fed mice normalised to cyclophilin. Values represent means \pm SEM. $n=8$ for WT and 11 for $G0s2^{-/-}$ mice on chow diet; $n=5$ for WT and 8 for $G0s2^{-/-}$ mice on HFD. * $p<0.05$, ** $p<0.01$, *** $p<0.0001$

(Fig. 3f). No changes were observed at the expression level of these key lipolytic genes (ESM Fig. 3).

We further analysed pre-adipocytes isolated from 3-week-old WT and $G0s2^{-/-}$ mice differentiated in vitro. Differentiated adipocytes were stimulated with the β -adrenergic agonist isoprenaline (10 $\mu\text{mol/l}$) for 2 h. Glycerol and NEFA levels were measured in media of the differentiated cells. Figure 4 shows increased basal and stimulated lipolysis as measured by glycerol release (Fig. 4a) and NEFA levels (Fig. 4b) in $G0s2^{-/-}$ adipocytes. In vivo lipolysis was also carried out in fasted 10–12 week WT and $G0s2^{-/-}$ mice treated with isoprenaline. As expected, treating mice with isoprenaline increased serum-free glycerol levels in all mice indicating hormone stimulated lipolysis; however, there were no significant differences between WT and $G0s2^{-/-}$ mice glycerol levels (data not shown).

To determine whether the decrease in adipocyte size is related to $G0s2$ regulation of adipocyte differentiation, gene expression analysis of adipocyte transcription factors and

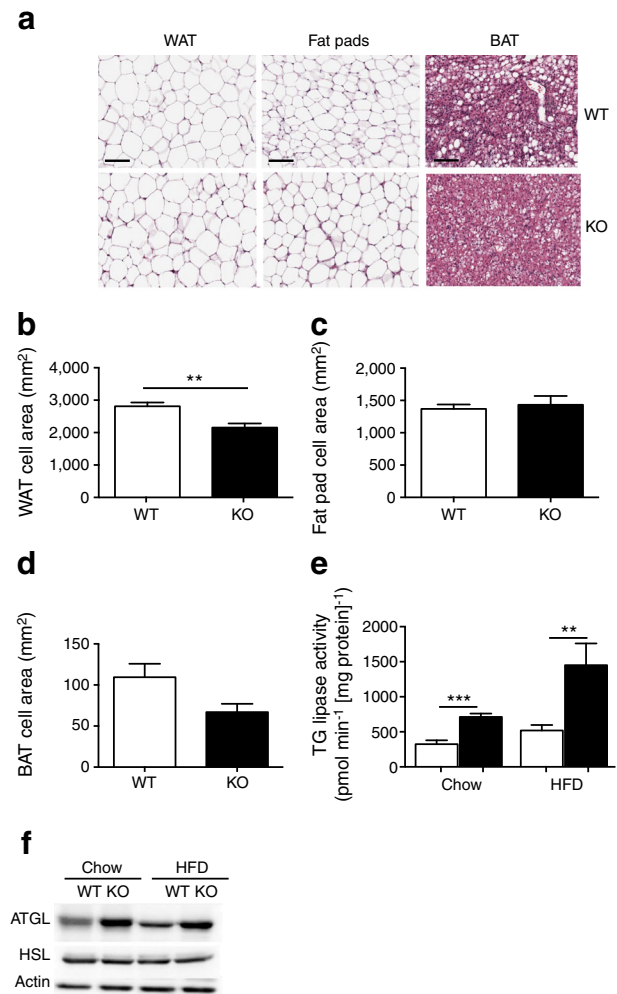


Fig. 3 Decreased adipocytes size and increased lipase activity in $G0s2^{-/-}$ (KO) mice. **(a)** H&E staining of WAT, fat pads and BAT of mice on an HFD for 22 weeks (scale bar, 100 μm). **(b)** Average WAT area, **(c)** fat pad area and **(d)** BAT area of WT (white bars) and KO (black bars) mice. **(e)** TG hydrolase activity measured in visceral fat extracts of male WT (white bars) and KO (black bars) mice. **(f)** Protein levels of ATGL and HSL in visceral lysates of WT and KO mice. Values represent means \pm SEM. $n=4$ per genotype for adipocyte area; $n=6$ per genotype for TG hydrolase activity and $n=4$ per genotype for protein levels. ** $p<0.01$, *** $p<0.001$

differentiation genes was performed [19–21]. Figure 4c shows no significant changes between genotypes, indicating that deletion of $G0s2$ does not interfere with adipocyte differentiation. Thus, the lean phenotype and decrease in adipocyte size observed in absence of $G0s2$ is likely to be due to elevated ATGL activity and enhanced lipolysis.

G0s2^{-/-} mice displayed improved glucose and insulin tolerance on high-fat feeding To examine whether insulin resistance developed in mice on the HFD, intraperitoneal glucose (IPGTT) and insulin (IPITT) tolerance tests were performed on overnight-fasted male WT and $G0s2^{-/-}$ mice (Fig. 5). On chow diet, glucose and insulin response curves were not different (Fig. 5a, c). However, in high-fat-fed mice, plasma

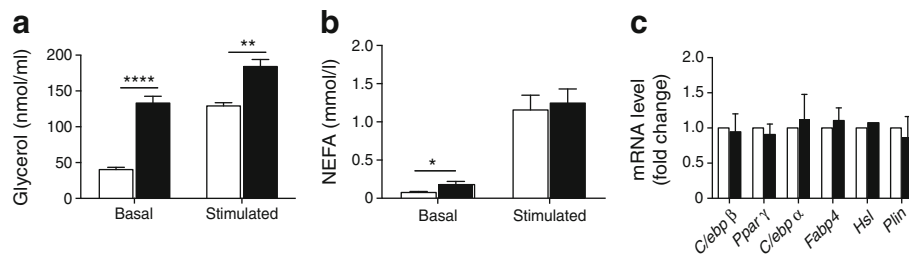


Fig. 4 Deletion of *G0s2* enhances lipolysis. In vitro lipolysis of differentiated adipocytes from 3-week-old mice under basal and isoprenaline-stimulated conditions. **(a)** Glycerol levels, **(b)** NEFA levels of WT (white

bars) and *G0s2*^{-/-} (KO) (black bars) mice ($n=9-10$ mice per condition). **(c)** Gene expression analysis of adipogenic differentiation markers normalised to cyclophilin. * $p<0.05$, ** $p<0.01$, **** $p<0.0001$

glucose levels were higher in WT mice, suggesting increased glucose tolerance in the knockout mice (Fig. 5b). Moreover, *G0s2*^{-/-} mice exhibited lower levels of hyperglycaemia in response to insulin load (Fig. 5d), suggesting that these mice are more insulin tolerant. On either diet, when IPITT or IPGTT were performed on female mice, no differences between genotypes were found (ESM Fig. 4a–d). Insulin levels during IPGTT in male mice are shown in ESM Fig. 4e.

Enhanced energy expenditure in *G0s2*^{-/-} mice *G0s2*^{-/-} mice are leaner and accumulate significantly less fat, suggesting enhanced energy expenditure. To further study this phenotype, mice fed either chow or HFD were placed in metabolism cages (Columbus Instruments, Columbus, OH, USA) for 4 days with free access to food and water. Oxygen consumption, activity and body temperature were recorded. Oxygen consumption measurements ($\dot{V}O_2$) showed an increase in *G0s2*^{-/-} mice both in light and dark cycles (about 20%);

however, the measurement was only statistically significant in dark cycles (Fig. 6a). No significant differences were observed in activity or food intake throughout the course of the metabolism cage analysis (Fig. 6b, c), confirming that the increased energy expenditure is not linked to physical activity or food intake, but is rather due to intrinsic changes in metabolism in *G0s2*^{-/-} mice.

Intriguingly, on chow diet, the respiratory quotient (RQ), which represents the ratio of ($\dot{V}CO_2/\dot{V}O_2$), was shifted towards 0.7 in *G0s2*^{-/-} mice, indicating that fat is a preferred substrate in these animals (Fig. 6d). The lower RQ is consistent with the *G0s2*^{-/-} animals having enhanced lipolysis and fat metabolism. The RQ values of WT and *G0s2*^{-/-} mice were nearly identical once animals were placed on a HFD since this forces the use of lipids in both groups (Fig. 6e).

Enhanced thermogenesis in *G0s2*^{-/-} mice Brown adipocytes, unlike white adipocytes, produce heat as a means to counteract hypothermia, obesity and diabetes. Brown fat has a high mitochondrial content and mitochondrial uncoupling protein 1 (UCP1) can be used to uncouple respiration and dissipate chemical energy as heat. Analysis of *G0s2*^{-/-} mice housed in metabolism cages, showed an increase in heat production (Fig. 7a, b) on 14 weeks of HFD conditions (Fig. 7b). mRNA and protein levels of ATGL, HSL and UCP1 were measured in BAT tissue and showed a slight increase in UCP1 levels under HFD conditions (ESM Fig. 5). These data prompted us to investigate the adaptation of *G0s2*^{-/-} mice to cold exposure. Mice (12 weeks old) on chow diet were housed at 4°C and their rectal temperature was recorded during the first 5 h and then at 30 h (Fig. 7c). *G0s2*^{-/-} mice had an approximately 0.7°C higher body temperature than WT mice. Moreover, abdominal temperature was measured at 30 h and was on average 0.8°C higher in *G0s2*^{-/-} animals (Fig. 7d). These data suggest that *G0s2*^{-/-} mice are overall more thermogenic and the heat generated is able to counteract obesity.

We next examined whether BAT molecular markers were increased in WAT of *G0s2*^{-/-} mice at normal and cold temperatures. HFD-fed *G0s2*^{-/-} mice expressed increased levels

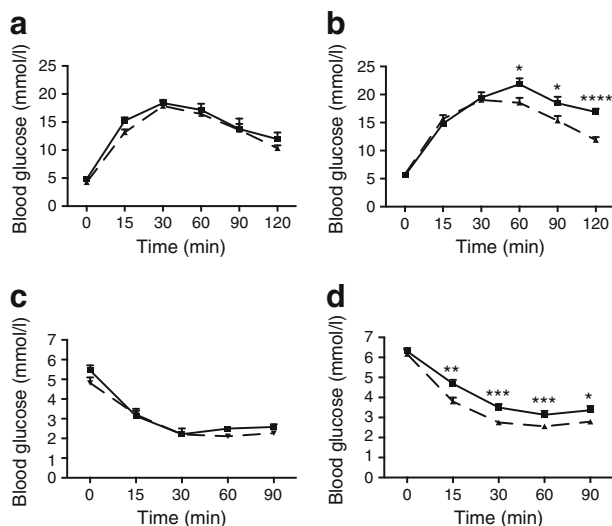
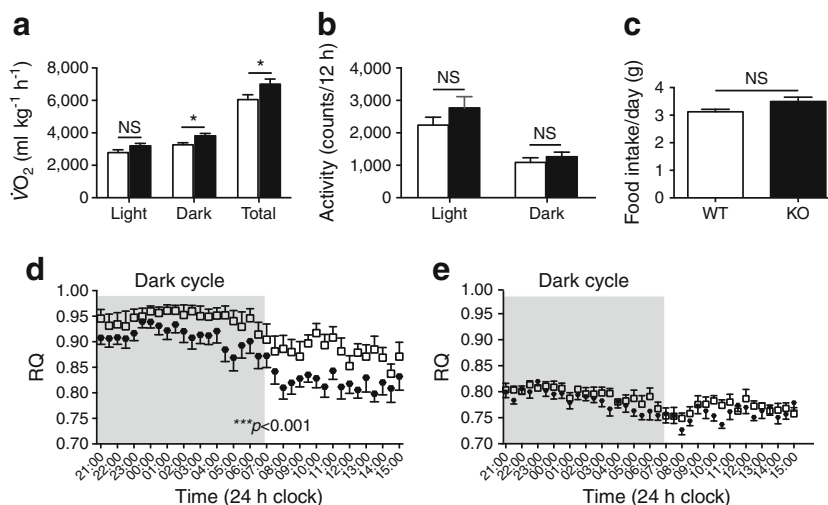


Fig. 5 Improved glucose and insulin sensitivity in *G0s2*^{-/-} (KO) male mice. Blood glucose levels during **(a, b)** IPGTT and **(c, d)** IPITT in fasted WT (black squares) and KO (black triangles) mice on **(a, c)** chow diet and **(b, d)** HFD. Values represent means±SEM. $n=8$ for WT and $n=13$ for KO mice. * $p<0.05$, ** $p<0.01$, *** $p<0.001$, **** $p<0.0001$

Fig. 6 Increased energy expenditure in *G0s2*^{-/-} (KO) mice. Mice were housed individually for 4 days in metabolism cages and fed either chow or HFD. (a) $\dot{V}O_2$ and (b) ambulatory activity of mice on HFD measured as counts per 12 h cycle. (c) Food intake on chow diet. WT (white bars) and KO (black bars). Respiratory quotient in WT (white squares) and KO (black hexagons) mice fed (d) chow or (e) HFD. Values represent means±SEM. *n*=7 per genotype. **p*<0.05; in (d) *p*<0.001 WT vs KO at all time points



of brown fat genes at normal temperature (Fig. 7e), and these increases were enhanced and significant under cold

temperature (4°C) (Fig. 7f). We observed an increase in the expression levels of key thermogenic genes, such as *Ucp1* and *Dio2*, in *G0s2*^{-/-} mice (Fig. 7e, f). This overall increase in selective brown fat genes in *G0s2*^{-/-} WAT suggests an overall browning of these tissues. In addition, there was a significant increase in genes that encode proteins for both mitochondrial and peroxisomal FA oxidation (Fig. 7g, h) such as *Cox8b*, *Acox*, *Pparα*, *Cpt1β*, *Pgc1α*, *Pgc1β* and *Ech1* in HFD-fed mice (Fig. 7h). These results suggest that the increased thermogenesis and browning of WAT are likely to be responsible for the enhanced energy dissipation in the knockout mice.

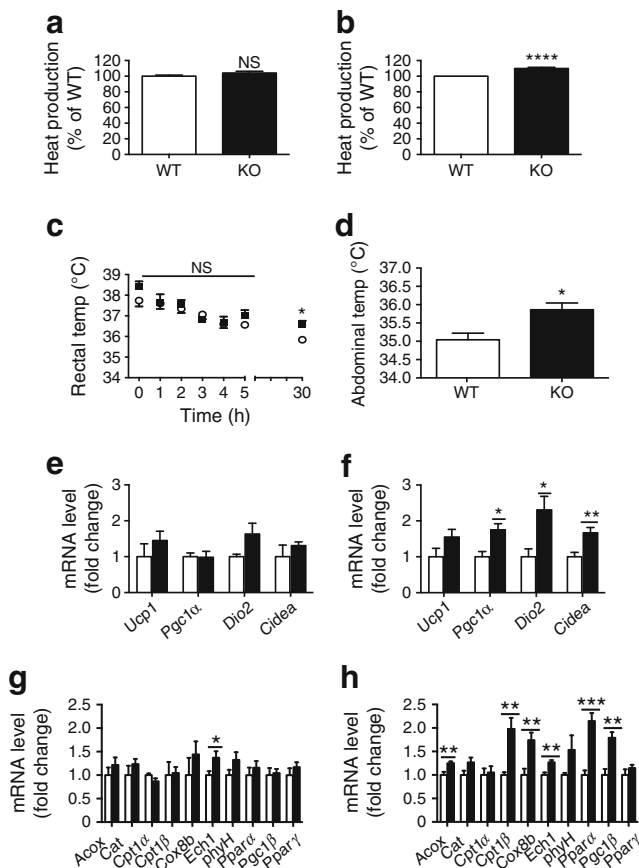


Fig. 7 Increased thermogenicity and oxidation in *G0s2*^{-/-} (KO) mice. Body temperature measured indirectly as heat production in metabolism cages of WT (white bars) and KO (black bars) mice on (a) chow and (b) HFD. (c, d) Rectal and abdominal temperatures of WT (white) and KO (black) mice on chow diet housed for 30 h at 4°C. (e–h) Expression levels of thermogenic and oxidation genes in WAT of WT (white bars) and KO (black bars) mice on HFD housed at (e, g) room temperature or (f, h) 4°C for 8 h. *n*=7–8 per genotype. **p*<0.05, ***p*<0.01, ****p*<0.001

Discussion

The current study demonstrates the role of *G0s2* as an in vivo regulator of lipase activity. Mice lacking *G0s2* expression had elevated TG hydrolase activity, were leaner and more resistant to HFD weight increase than WT littermates. In addition, lipolysis was enhanced in differentiated adipocytes isolated from *G0s2*^{-/-} mice and markedly enhanced in response to stimulation by isoprenaline. *G0s2*^{-/-} mice had reduced TG levels in the liver, and both WAT and BAT cells were smaller than those in WT controls. In addition, *G0s2*^{-/-} mice had improved glucose tolerance and insulin sensitivity and were more thermogenic due to enhanced fat catabolism. Taken together, the data provide strong evidence that G0S2 is a key regulator of lipid metabolism in vivo.

Our results are consistent with recent findings in a transgenic mouse model in which *Atgl* (also known as *Pnpl2*) was overexpressed in adipose tissue causing reduced TG content and enhanced lipolysis [22]. By contrast, *Atgl*^{-/-} mice accumulate large amounts of fat in multiple tissues and die at around 12 weeks of age [23]. Correlative studies have indicated that the G0S2 regulatory effects on lipid metabolism

may also extend to humans. For example, fasting in humans was shown to reduce G0S2 levels and elevate ATGL [24].

Despite the enhanced lipolysis and decreased TG levels in tissues and sera, serum NEFA levels in the *G0s2*^{-/-} mice were surprisingly unchanged. Moreover, we noticed that on both diets, NEFA levels in the liver and sera of *G0s2*^{-/-} mice tended to be even lower than those of WT mice, suggesting enhanced fat use/uptake. Under normal conditions, a balance between hydrolysis and use/uptake regulates NEFA levels by peripheral tissues. Many factors can regulate levels of NEFA in serum. Thus, the lack of increased serum NEFA levels suggests alternative mechanisms by which NEFA are used. We have observed enhanced glucose tolerance and insulin sensitivity in *G0s2*^{-/-} mice, which could suggest increased FA uptake by peripheral tissues. Oxidation and/or re-esterification of NEFA are potential mechanisms by which NEFA are used. NEFA can also be recycled back to DAG or MAG through the TG/NEFA cycle bypassing the TG step, perhaps favouring shorter cycles to ensure the availability of different signalling intermediates (discussed in [25]).

G0s2^{-/-} mice had higher body temperatures, increased oxygen consumption and lower RQ ratio, indicating more fat usage. Moreover, knockout mice were more tolerant to cold temperatures and maintained higher body temperatures than WT mice. We speculate that elevated fat oxidation, and possibly uncoupling, are the mechanisms by which *G0s2*^{-/-} mice are able to use fat more rapidly and thus generate heat. Increased expression of brown fat-like genes in WAT of *G0s2*^{-/-} mice further argues for enhanced uncoupling and energy dissipation in these animals as a means to counteract obesity. Our findings are in agreement with other mouse models that display enhanced FA oxidation and decreased serum NEFA levels [26, 27]. Overexpression of *Ucp1* in WAT of mice for example, resulted in enhanced uncoupling, leanness and increased FA oxidation [26] with improved insulin sensitivity [28]. Prolonged cold exposure is known to induce WAT into a BAT-like state, a process termed browning [29, 30]. Interestingly, a recent study demonstrated that in response to cold exposure, expression levels of ATGL became elevated, whereas levels of G0S2 were decreased in fat deposits of SvEv mice [31]. These changes in gene expression would enhance the lipolytic potential of adipocytes. Our findings suggest that lack of G0S2 activity is able to accelerate the process of browning. Inducing the browning of WAT has been proposed as a potential therapy for obesity and type 2 diabetes and our findings suggest that G0S2 may be an effective therapeutic target in this regard [32].

Our study is the first to show that G0S2 regulates WAT browning by acting as a negative regulator of lipolysis. A recent report by Zhang et al has also described the phenotype of *G0s2*^{-/-} mice [33]. Both our study and that of Zhang et al [33] show that *G0s2*^{-/-} mice are leaner and resistant to HFD feeding in 129SvEv and C57BL/6J genetic background,

respectively. Both studies show a decrease in TG accumulation in the liver and enhanced lipase activity in visceral fat and liver. However, in our study, effects of G0S2 on lipolysis, resistance to HFD obesity, and improvement in glucose and insulin sensitivity were more significant in male than in female *G0s2*^{-/-} mice, whereas in the study by Zhang et al female mice displayed greater resistance to HFD-induced obesity [33]. These variations may be due to the different mouse strains used in the two studies or to metabolic adaptation/compensation in female 129SvEv mice in our study. Sex differences have been previously reported to have different effects in metabolic studies [34]. Our data are also in agreement with a recently published report of *G0s2* overexpression in adipocytes [35]. In this model, overexpression of *G0s2* in adipocytes rendered the mice unable to maintain their body temperature at 4°C, probably due to increased fat deposition in these mice. A new report also showed G0S2 regulation of thermogenesis and an increase in brown-like and oxidation genes in BAT of *G0s2*^{-/-} mice [36].

In conclusion, our study highlights the role of G0S2 in whole body lipid metabolism and suggests that G0S2 may have a role in metabolic disorders such as obesity, insulin resistance and type 2 diabetes.

Acknowledgements We thank S. Hardy (Goodman Cancer Research Centre, McGill University, Montreal, QC, Canada) for reading the manuscript and A. L. Loy (Goodman Cancer Research Centre) for assistance with mouse experiments.

Funding This work was supported by grants from the CIHR (MOP-115195) and Cancer Research Society (CRS) to JGT and NIH grant AI075118 to MAK.

Duality of interest The authors declare that there is no duality of interest associated with this manuscript.

Contribution statement WE-A, MAK, SK, MLT and JGT designed the study. WE-A, KE-K, JY, IG, and NH contributed to the acquisition and interpretation of data. AHM, MM, OM and DA analysed the data. WE-A and JGT wrote the manuscript with all other authors contributing to the review and revision of intellectual content. All authors approved the final manuscript. JGT is the guarantor of this work.

References

1. Miranda PJ, DeFronzo RA, Califf RM, Guyton JR (2005) Metabolic syndrome: definition, pathophysiology, and mechanisms. *Am Heart J* 149:33–45
2. Reaven GM (1988) Banting lecture 1988. Role of insulin resistance in human disease. *Diabetes* 37:1595–1607
3. Jenkins CM, Mancuso DJ, Yan W, Sims HF, Gibson B, Gross RW (2004) Identification, cloning, expression, and purification of three novel human calcium-independent phospholipase A2 family members possessing triacylglycerol lipase and acylglycerol transacylase activities. *J Biol Chem* 279:48968–48975
4. Villena JA, Roy S, Sarkadi-Nagy E, Kim KH, Sul HS (2004) Desnutrin, an adipocyte gene encoding a novel patatin domain-containing protein, is induced by fasting and glucocorticoids:

- ectopic expression of desnutrin increases triglyceride hydrolysis. *J Biol Chem* 279:47066–47075
5. Zimmermann R, Strauss JG, Haemmerle G et al (2004) Fat mobilization in adipose tissue is promoted by adipose triglyceride lipase. *Science* 306:1383–1386
 6. Holm C, Kirchgesner TG, Svenson KL et al (1988) Hormone-sensitive lipase: sequence, expression, and chromosomal localization to 19 cent-q13.3. *Science* 241:1503–1506
 7. Holm C, Osterlund T, Laurell H, Contreras JA (2000) Molecular mechanisms regulating hormone-sensitive lipase and lipolysis. *Annu Rev Nutr* 20:365–393
 8. Boden G, Shulman GI (2002) Free fatty acids in obesity and type 2 diabetes: defining their role in the development of insulin resistance and beta-cell dysfunction. *Eur J Clin Invest* 32(Suppl 3):14–23
 9. Yang X, Lu X, Lombes M et al (2010) The G₀/G₁ switch gene 2 regulates adipose lipolysis through association with adipose triglyceride lipase. *Cell Metab* 11:194–205
 10. Lu X, Yang X, Liu J (2010) Differential control of ATGL-mediated lipid droplet degradation by CGI-58 and G0S2. *Cell Cycle* 9:2719–2725
 11. Zandbergen F, Mandard S, Escher P et al (2005) The G₀/G₁ switch gene 2 is a novel PPAR target gene. *Biochem J* 392:313–324
 12. Welch C, Santra MK, El-Assaad W et al (2009) Identification of a protein, G0S2, that lacks Bcl-2 homology domains and interacts with and antagonizes Bcl-2. *Cancer Res* 69:6782–6789
 13. Ma L, Robinson LN, Towle HC (2006) ChREBP*MIx is the principal mediator of glucose-induced gene expression in the liver. *J Biol Chem* 281:28721–28730
 14. Le Bacquer O, Petroulakis E, Paglialunga S et al (2007) Elevated sensitivity to diet-induced obesity and insulin resistance in mice lacking 4E-BP1 and 4E-BP2. *J Clin Invest* 117:387–396
 15. Almind K, Kahn CR (2004) Genetic determinants of energy expenditure and insulin resistance in diet-induced obesity in mice. *Diabetes* 53:3274–3285
 16. Kulkarni RN, Almind K, Goren HJ et al (2003) Impact of genetic background on development of hyperinsulinemia and diabetes in insulin receptor/insulin receptor substrate-1 double heterozygous mice. *Diabetes* 52:1528–1534
 17. Nomura DK, Long JZ, Niessen S, Hoover HS, Ng SW, Cravatt BF (2010) Monoacylglycerol lipase regulates a fatty acid network that promotes cancer pathogenesis. *Cell* 140:49–61
 18. Schweiger M, Paar M, Eder C et al (2012) G₀/G₁ switch gene-2 regulates human adipocyte lipolysis by affecting activity and localization of adipose triglyceride lipase. *J Lipid Res* 53:2307–2317
 19. Brun RP, Kim JB, Hu E, Altiock S, Spiegelman BM (1996) Adipocyte differentiation: a transcriptional regulatory cascade. *Curr Opin Cell Biol* 8:826–832
 20. Gregoire FM, Smas CM, Sul HS (1998) Understanding adipocyte differentiation. *Physiol Rev* 78:783–809
 21. Rosen ED, MacDougald OA (2006) Adipocyte differentiation from the inside out. *Nat Rev Mol Cell Biol* 7:885–896
 22. Ahmadian M, Duncan RE, Varady KA et al (2009) Adipose overexpression of desnutrin promotes fatty acid use and attenuates diet-induced obesity. *Diabetes* 58:855–866
 23. Haemmerle G, Lass A, Zimmermann R et al (2006) Defective lipolysis and altered energy metabolism in mice lacking adipose triglyceride lipase. *Science* 312:734–737
 24. Nielsen TS, Vendelbo MH, Jessen N et al (2011) Fasting, but not exercise, increases adipose triglyceride lipase (ATGL) protein and reduces G₀/G₁ switch gene 2 (G0S2) protein and mRNA content in human adipose tissue. *J Clin Endocrinol Metab* 96:E1293–E1297
 25. Prentki M, Madiraju SR (2008) Glycerolipid metabolism and signaling in health and disease. *Endocr Rev* 29:647–676
 26. Kopecky J, Clarke G, Enerback S, Spiegelman B, Kozak LP (1995) Expression of the mitochondrial uncoupling protein gene from the aP2 gene promoter prevents genetic obesity. *J Clin Invest* 96:2914–2923
 27. Orci L, Cook WS, Ravazzola M et al (2004) Rapid transformation of white adipocytes into fat-oxidizing machines. *Proc Natl Acad Sci U S A* 101:2058–2063
 28. Yamada T, Katagiri H, Ishigaki Y et al (2006) Signals from intra-abdominal fat modulate insulin and leptin sensitivity through different mechanisms: neuronal involvement in food-intake regulation. *Cell Metab* 3:223–229
 29. Petrovic N, Walden TB, Shabalina IG, Timmons JA, Cannon B, Nedergaard J (2010) Chronic peroxisome proliferator-activated receptor gamma (PPARgamma) activation of epididymally derived white adipocyte cultures reveals a population of thermogenically competent, UCP1-containing adipocytes molecularly distinct from classic brown adipocytes. *J Biol Chem* 285:7153–7164
 30. Wu J, Bostrom P, Sparks LM et al (2012) Beige adipocytes are a distinct type of thermogenic fat cell in mouse and human. *Cell* 150:366–376
 31. Barneda D, Frontini A, Cinti S, Christian M (2013) Dynamic changes in lipid droplet-associated proteins in the “browning” of white adipose tissues. *Biochim Biophys Acta* 1831:924–933
 32. Wu J, Cohen P, Spiegelman BM (2013) Adaptive thermogenesis in adipocytes: is beige the new brown? *Genes Dev* 27:234–250
 33. Zhang X, Xie X, Heckmann BL, Saarinen AM, Czyzyk TA, Liu J (2014) Targeted disruption of G₀/G₁ switch gene 2 enhances adipose lipolysis, alters hepatic energy balance, and alleviates high fat diet-induced liver steatosis. *Diabetes* 63:934–946
 34. Peyot ML, Nolan CJ, Soni K et al (2004) Hormone-sensitive lipase has a role in lipid signaling for insulin secretion but is nonessential for the incretin action of glucagon-like peptide 1. *Diabetes* 53:1733–1742
 35. Heckmann BL, Zhang X, Xie X et al (2014) Defective adipose lipolysis and altered global energy metabolism in mice with adipose overexpression of the lipolytic inhibitor G₀/G₁ switch gene 2 (G0S2). *J Biol Chem* 289:1905–1916
 36. Ma T, Lopez-Aguilar AG, Li A et al (2014) Mice lacking G0S2 are lean and cold-tolerant. *Cancer Biol Ther* 15:643–650